

Fragility of underground pipeline under high levels of ground motion

Yasuko Kuwata, Shiro Takada, Yuki Tanaka, Hiroaki Miyazaki and Yoshimitsu Komatsu

ABSTRACT

Damage estimation relationships have been proposed based on seismic ground motions and pipeline damage records from past earthquakes as a technique for understanding damage in future seismic hazards. This kind of relationship is formulated by correcting the standard damage relationship shown by the amount of damage from seismic ground motion with coefficients such as pipe materials and ground conditions. However, the existing relationship is based on the actual earthquake data, and has not yet been verified by numerical analysis. In addition, there is little data on pipeline damage by high-level seismic ground motion from the 1995 Kobe earthquake, and we cannot compare those in the other earthquakes. Therefore, this study was conducted to analyse the damage tendency by using the seismic response analysis of a pipeline under high-level ground motion with the aid of the discrete element method (DEM), which can express slipping out and breaking of the pipeline joint. The damage tendency to the pipeline was evaluated relatively by giving the characteristic of the pipe material and joint.

Key words | damage rate, fragility, joint mechanics, seismic ground motion, seismic response analysis, underground pipeline

Yasuko Kuwata (corresponding author)
Yuki Tanaka
Department of Civil Engineering,
Kobe University,
Rokkodai 1, Nada, Kobe 657-8501,
Japan
Tel.: +81 78 803 6047
Fax: +81 78 803 6047
E-mail: kuwata@kobe-u.ac.jp

Shiro Takada
Faculty of Civil Engineering, Engineering College,
University of Tehran,
Keshavarz Blvd, No. 268,
Tehran 1417633861,
Iran

Hiroaki Miyazaki
Yoshimitsu Komatsu
Engineering Division,
Osaka City Waterworks Bureau,
Nanko-Kita, Suminoe,
Osaka 559-8558,
Japan

INTRODUCTION

Seismic damage estimation for underground pipelines has been done by using damage estimation formulae (so-called fragility relationship) obtained by statistical data from past earthquakes (Takada *et al.* 2001). Isoyama *et al.* (1998) proposed a fragility relationship for ductile cast iron (DIP) and grey cast iron (CIP) pipelines based on the damage data during the 1995 Kobe earthquake, which shows the pipe damage increases exponentially according to ground velocity. Hosokawa *et al.* (2001) also proposed a fragility relationship which shows that the damage ratio of low pressure gas pipelines reaches a constant when the ground motion becomes more than 100 cm s^{-1} .

However, any numerical calculation for the pipeline damage formulae, which can be applicable to the high-level ground motion, does not exist so far. There is limited data on pipeline damage by high-level seismic ground motion from

the 1995 Kobe earthquake (JWWA 1996), and we cannot compare those of the other earthquakes. Recent seismic ground motion records show a higher level of ground motion than 100 cm s^{-1} . This study is conducted to analyse the damage tendency by using the seismic response analysis of a pipeline under high-level ground motion with the aid of DEM, which can express slipping out and breaking of the pipeline joint. The numerical result is evaluated to compare with the empirical relationship between pipeline damage and ground motion (Takada *et al.* 2003).

METHODS

Analysis model

DEM (discrete element method) is an analytical method to treat the motion of a set of particles as non-continuous

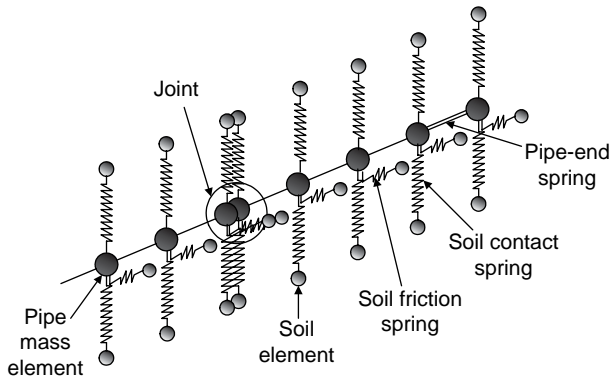


Figure 1 | Pipeline model by DEM.

media. Three-dimensional equilibrium equations can be shown as follows:

$$\ddot{x}_i + \alpha \dot{x}_i = \frac{F_i}{m_i} + g \tag{1}$$

$$\ddot{\omega}_i + \alpha \dot{\omega}_i = \frac{M_i}{I_i} \tag{2}$$

where, x_i is coordinate of particle, α is a damping constant, F_i is total force acting on particle, m_i is mass of particle, g is gravity acceleration, ω_i is rotation of particle, M_i is total moment of particle and I_i is inertia moment of particle.

Figure 1 shows an underground pipeline modelled by DEM. The pipe is modelled by concentrated mass and beam and the pipe joint is expressed by specific spring between two particles, which allows three-dimensional behaviour. Soil spring means the restrained force with slippage between the pipe and ground. Figure 2 is a targeted straight pipeline model with 100 m length of diameter $\Phi 100$ and 150 mm. One segment of the pipeline is 4 and 5 m for the $\Phi 100$ and $\Phi 150$ mm diameter pipeline, respectively.

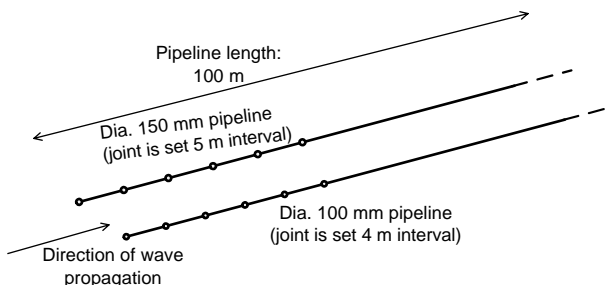


Figure 2 | Analytical model of pipeline.

Table 1 | Features of targeted pipes

Pipe	N. Diameter (mm)	Diameter (mm)	t (mm)	E (N mm ⁻²)	σ_t (N mm ⁻²)	σ_c (N mm ⁻²)
DIP	100	118	6	157,000	420	840
	150	169	6			
CIP	100	114	4.5	155,000	200	730
	150	159	4.5			
PVC	100	114	7.1	2,700	52	65
	150	165	9.6			

The end of the pipeline is set to free conditions to avoid stress concentrations.

Pipe joint targeted

Materials of the pipe are DIP (ductile cast iron pipe), CIP (grey cast iron pipe) and PVC (polyvinyl pipe), whose features are listed in Table 1. Bending characteristics for DIP and CIP are determined in terms of EI. For PVC, M- Φ relations are introduced as shown in Figure 3. Soil spring is set with reference to JGA (Japan Gas Association 1982) specification as listed in Table 2.

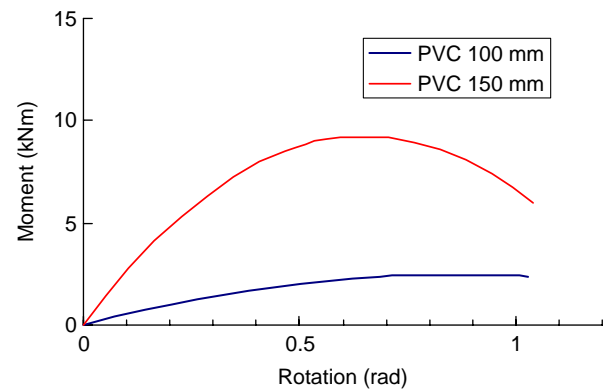


Figure 3 | PVC bending characteristics.

Table 2 | Soil spring property

Pipe	Soil spring k (N cm ⁻³)		
	Transverse	Axial	Yield displacement (cm)
DIP	13.1	5.9	0.5
CIP	13.5	5.9	0.5
PVC	13.5	2.9	0.5

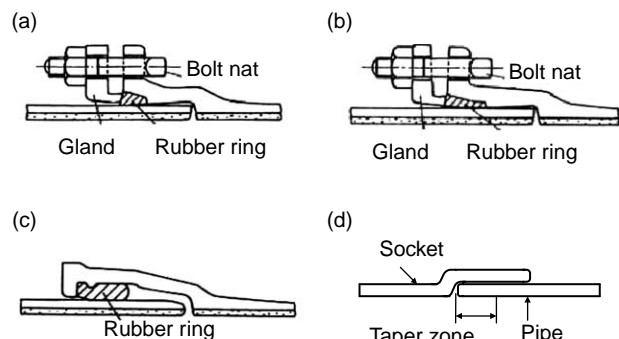


Figure 4 | Configuration of joint mechanics: (a) DIP-A type; (b) DIP-K type; (c) DIP-T type; (d) PVC-TS type.

A, K and T-type joints specified by JWWA (Japan Water Works Association 1997) are analysed for DIP pipelines (Figure 4). Damage of these pipelines is defined as the state where displacement or rotation angle of the joints reaches the ultimate values.

Figure 5 shows the ultimate tension and compression displacements and also rotation angle in each type of DIP joint. Tensile property is set in consideration with the slipping displacement of the joint and friction of the rubber ring. For the compression force, the maximum force is determined as 350 kN since the joint has compression failure under both compression and bending force. The bending relationship refers to the experimental tests of Gas SGM joint. The joint types A and K for bending property are assumed to be the same. The joint characteristics of CIP are obtained by experiments for gas CIP pipes. These joint behaviours are shown in Figure 6. The joint of the PVC pipe is a tapered joint, known as a TS joint. The failure strain is set as 0.2% for tension and compression.

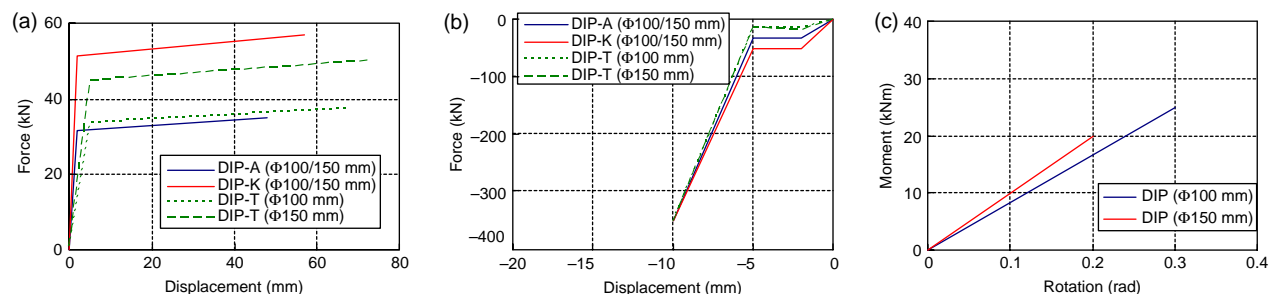


Figure 5 | DIP joint characteristics for A, K and T types: (a) tension; (b) compression; (c) rotation.

Ground motion

In the seismic response analyses by DEM, the accelerogram of strong ground motion observed at Takatori station in the 1995 Kobe earthquake is used for the input as shown in Figure 7. The velocity amplitude of the records is converted to eight levels to check the change of response behaviour. Seismic ground motion in the NS component is assigned to the pipe axis, whereas that in the EW component is transverse to it.

RESULTS AND DISCUSSION

Verification of analysis

First, the response of the pipe joint is checked changing the propagation velocity of the wave for the case of the DIP-K type jointed pipeline with 100 mm diameter. The joint displacement calculated by the DEM is compared with that estimated by the ground strain and pipe length as shown in Figure 8. The joint displacement is checked at joint (a) 24 m from the end and joint (b) at the centre of pipeline.

The compressive displacement at every joint is over an allowable compressive displacement of the joint, which means the joints have high rigidity owing to collision in adjacent pipe segments. Some joints have pulling-out behaviour under the low speed of wave propagation. However, the results indicate a fairly good agreement under the high-level ground motions. Then we have to check the behaviour not only as the average value of the joints, but the behaviour of each joint.

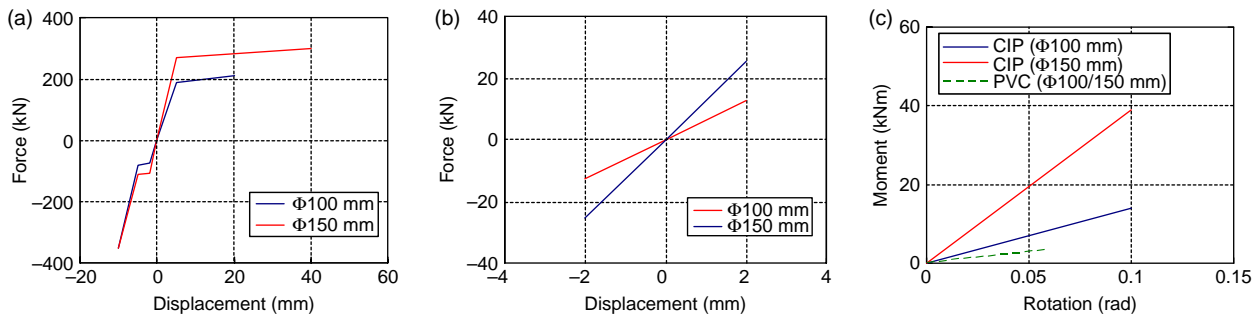


Figure 6 | Joint characteristics for CIP-C and PVC-TS: (a) axial CIP-C; (b) axial PVC-TS; (c) bending CIP-C/PVC-TS.

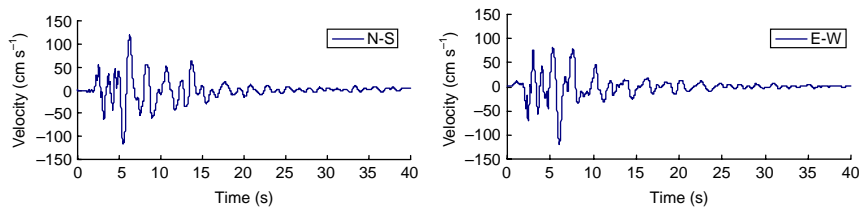


Figure 7 | Seismic ground motion inputted (left: NS component, right: EW component).

Fragility rate of joint

Next, the joint behaviour and its damage tendency are examined for 10 models of pipelines with various types of joint and diameter inputted by amplitude-arranged eight ground motions. The wave propagation velocity is 100 m s^{-1} for all cases. If the joint displacement reaches one of the allowable values of tension, compression and rotation, the joint is determined as failed.

Here, the fragility ratio of joints depending on the maximum ground velocity F_r (V_{\max}) is defined by:

$$F_r(V_{\max}) = \frac{J_f}{J} \times 100 \quad (3)$$

Here, F_r is the fragility rate of joint (%), J_f is the number of failure joint and J is the total number of joints.

The location of the failure joint and its damaged time at different level ground motions are analysed for the model of $\Phi 100$ pipeline with DIP-K type joint. In the case of ground motion with $V_{\max} = 90 \text{ cm s}^{-1}$, compression failure starts at three joints. This damage pattern is the same as the models of $\Phi 100$ pipeline with DIP-A and T type joints. In the case of $V_{\max} = 170 \text{ cm s}^{-1}$, the joint has a failure at the peak amplitude of ground motion and the joint, which is far from the first failed joint, was pulled out. As the inputted ground

motion level becomes high, the tension failure at joints increases. This failure pattern is affected by the inputted ground motion. The process of joint failure differs by the ground motion.

Figure 9 shows the process of pipe failure for the model of $\Phi 150$ pipeline with DIP-K type joint. The failure patterns in the case of $V_{\max} = 30 \text{ cm s}^{-1}$ are compression failure at joints, and they are the same in the models of pipeline with DIP-A and T type joints. When V_{\max} is over 90 cm s^{-1} , the joints pulled out at the first time. Similarly to $\Phi 100$ pipeline, as the inputted ground motion level becomes high, the tension failure at joints increases.

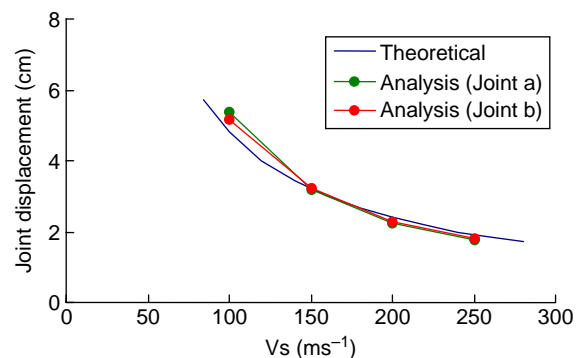


Figure 8 | Comparison of theory and numerical results ($V_{\max} = 120 \text{ cm s}^{-1}$).

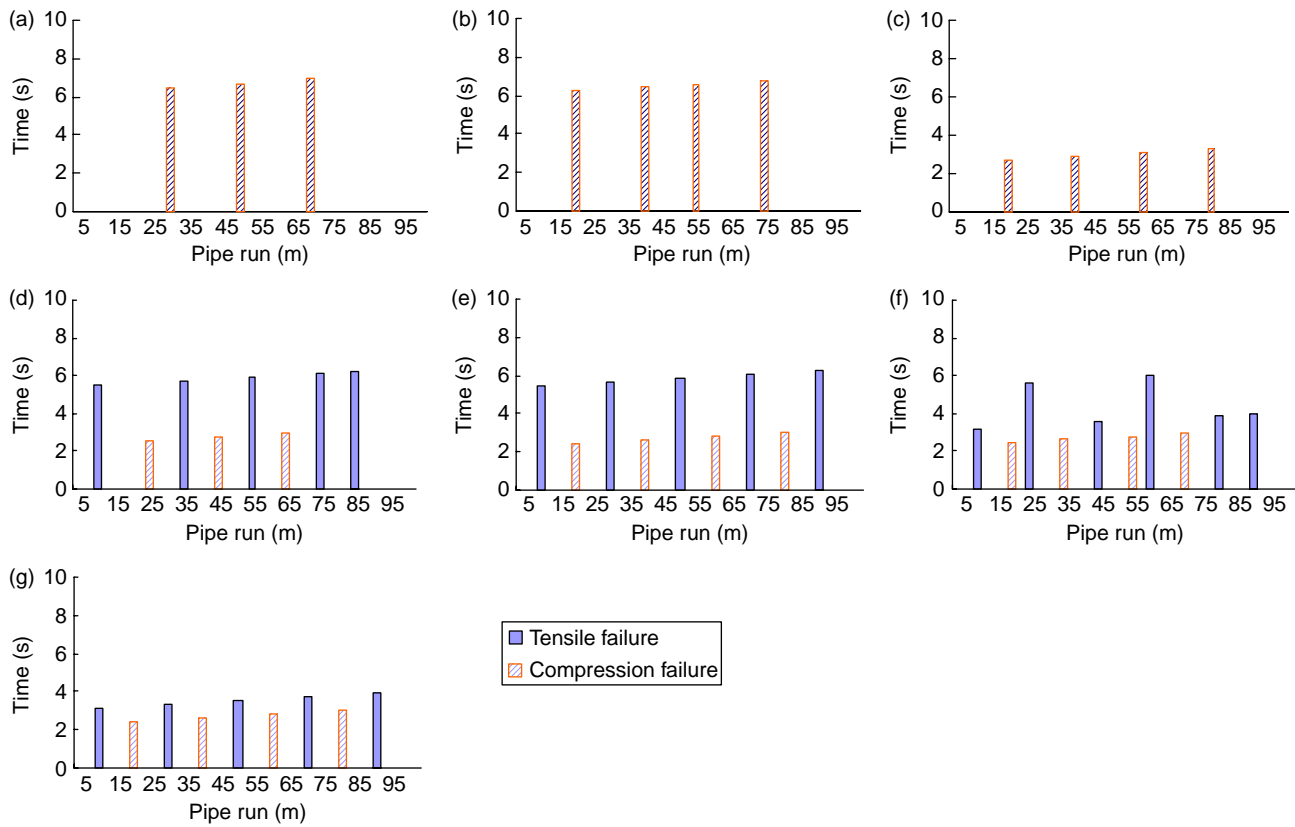


Figure 9 | DIP-K ($\Phi 150$ mm) joint failure hysteresis at the computation time: (a) $V_{max} = 30 \text{ cm s}^{-1}$; (b) $V_{max} = 50 \text{ cm s}^{-1}$; (c) $V_{max} = 90 \text{ cm s}^{-1}$; (d) $V_{max} = 120 \text{ cm s}^{-1}$; (e) $V_{max} = 150 \text{ cm s}^{-1}$; (f) $V_{max} = 170 \text{ cm s}^{-1}$; (g) $V_{max} = 190 \text{ cm s}^{-1}$.

The relation between the maximum ground velocity V_{max} and $F_r(V_{max})$ gives the fragility of the joints for each pipeline. **Figure 10** shows fragility relations of $\Phi 100$ pipeline for various types of joint of DIP, CIP and PVC. For the smaller amplitude of ground motion more than 120 cm s^{-1} ,

the DIP-T type joint has a lower failure ratio due to the larger allowable expansion displacement of 67 mm. For larger velocity amplitude of 150 cm s^{-1} , the joints with higher rigidity have less damage. A similar failure rate in the high-level ground motion is caused due to process of joint

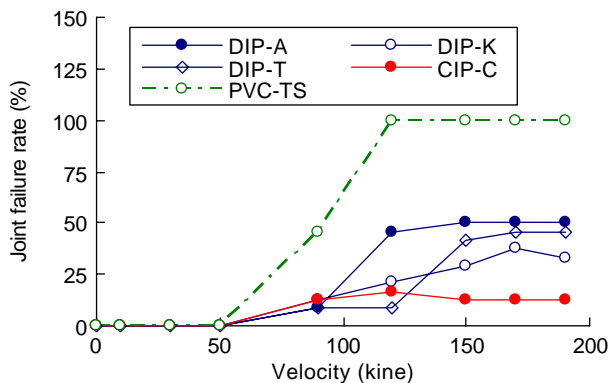


Figure 10 | Fragility relation of joint ($\Phi 100$ mm).

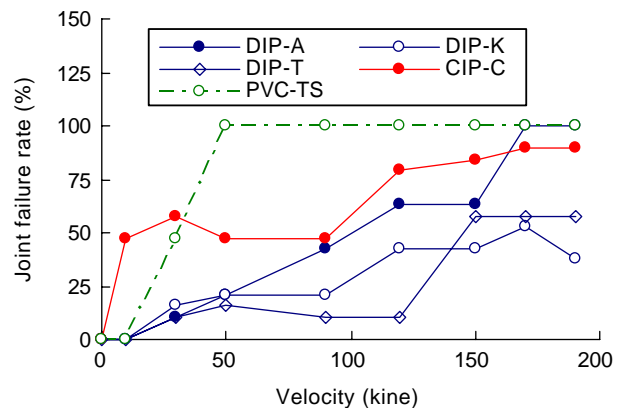


Figure 11 | Fragility relation of joint ($\Phi 150$ mm).

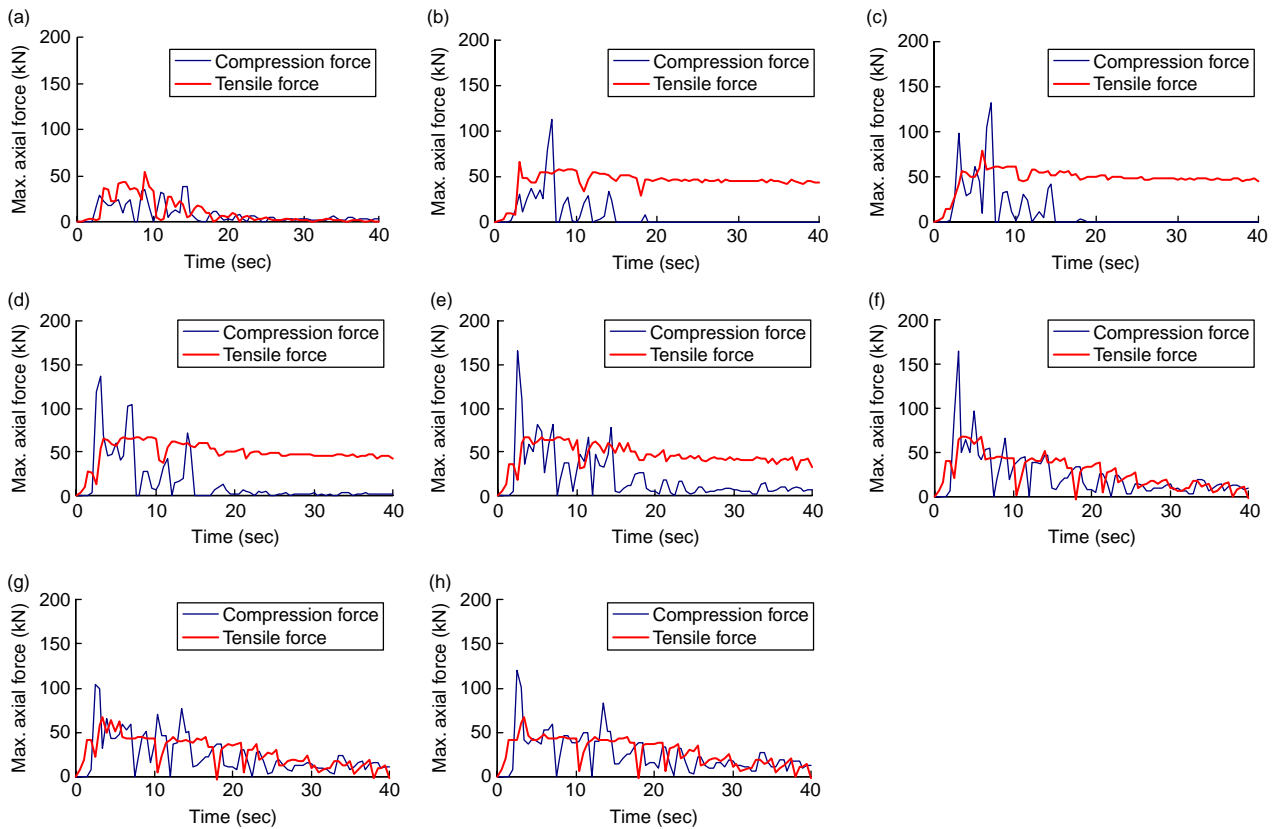


Figure 12 | Maximum axial force of pipeline (DIP-K, $\Phi 150$ mm): (a) $V_{\max} = 10 \text{ cm s}^{-1}$; (b) $V_{\max} = 30 \text{ cm s}^{-1}$; (c) $V_{\max} = 50 \text{ cm s}^{-1}$; (d) $V_{\max} = 90 \text{ cm s}^{-1}$; (e) $V_{\max} = 120 \text{ cm s}^{-1}$; (f) $V_{\max} = 150 \text{ cm s}^{-1}$; (g) $V_{\max} = 170 \text{ cm s}^{-1}$; (h) $V_{\max} = 190 \text{ cm s}^{-1}$.

failure as mentioned above. The PVC-TS type pipe has flexible material to resist up to $V_{\max} = 30 \text{ cm s}^{-1}$, whereas it is subjected to breakage in every joint location for the ground motion more than 120 cm s^{-1} .

Figure 11 shows the fragility relation for $\Phi 150$ mm pipelines. The tendency of damage rate for each type of joint is very different compared with $\Phi 100$ mm pipelines shown in Figure 10. CIP shows low reliability from the smaller velocity amplitude of ground motion. Velocity amplitude is just 10 cm s^{-1} when the CIP joint starts to be broken, whereas the PVC-TS type starts being broken at 30 cm s^{-1} . The larger diameter pipe is easier to break in compressive behaviour compared with smaller diameter pipelines because of the joint characteristics.

Fragility rate of pipe body

As the next step, the axial force is examined. Figure 12 shows the relation of maximum compression force and

tensile force of $\Phi 100$ pipeline of DIP-K type joint with respect to time. When the amplitude of the input ground motion is high, the maximum compression force is at its peak. Meanwhile the maximum tensile force is not as large as the compression force.

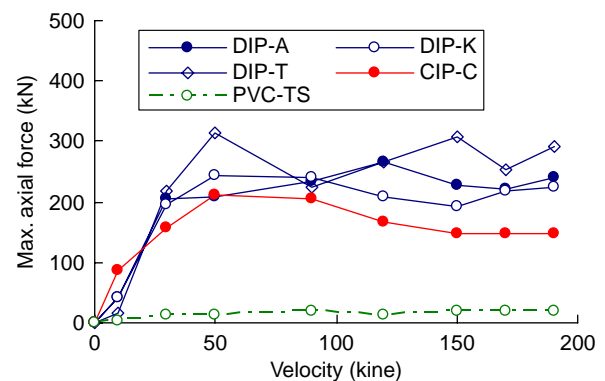


Figure 13 | Axial force relation ($\Phi 100$ mm).

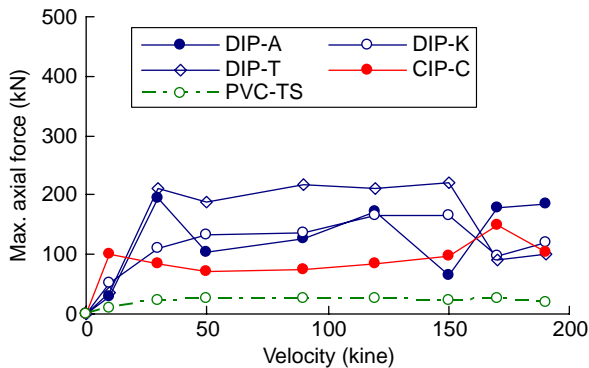


Figure 14 | Axial force relation ($\Phi 150$ mm).

Figures 13 and 14 show the relationships between ground velocity amplitude and maximum axial force in the pipeline. The maximum axial force shows its peak value at almost 50 cm s^{-1} and does not increase more for larger amplitudes in every type of pipeline. The pipeline resists ground motions by pipe displacement for tension force and by joint rigidity for compressive forces. Then these maximum axial forces are corresponding to compressive forces. Pulling out of DIP-T type pipeline causes the decrease of axial forces at 90 cm s^{-1} .

Fragility rate of pipeline

We have discussed the damage to pipe joints and axial force of pipe body separately in the above explanation. Next, the damage rate of pipeline (pipe fragility relationship) is defined as an average value of the joint damage ratio and ratio of the axial force to allowable axial force of the pipe body. Figures 15 and 16 show the pipe fragility relationships related to ground velocity. The damage

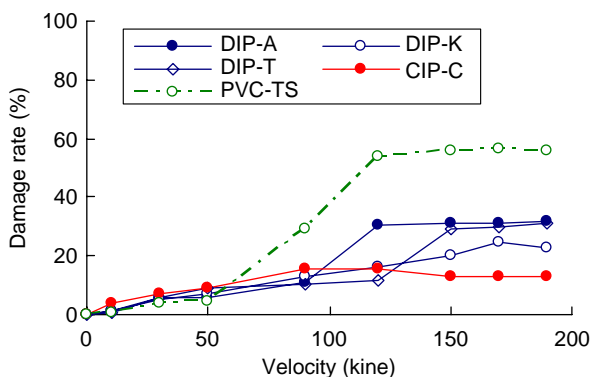


Figure 15 | Damage rate of pipeline ($\Phi 100$ mm).

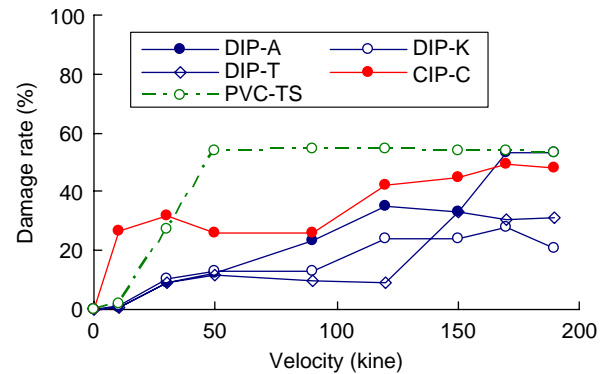


Figure 16 | Damage rate of pipeline ($\Phi 150$ mm).

rate shows the tendency for constant values for higher levels of ground amplitude, which is in agreement with the actual damage during the Kobe earthquake as stated in JWWA (1996) and Takada *et al.* (2001).

CONCLUSIONS

The results obtained would be some what changed under the assumed parameters in DEM analyses. However, it becomes clear that we can evaluate the pipe fragility relationship numerically even in the meaning of relative evaluation by giving pipe material and joint characteristics. Moreover, this study has revealed that the pipeline failure under a high level of ground motion follows the discontinuous damage process of joints and the pipe fragility relationship becomes constant owing to the limitation of the axial force applied to the pipeline.

The following are the results obtained by the present numerical analyses:

- Expansion and compressive behaviour of pipe joints strongly depends on the ground strain. Numerical calculation results for pipe joint displacements are mostly proportional to theoretical results. However, numerical calculation results show higher values than theoretical ones owing to complicated joint behaviour in each one.
- The proposed DEM calculation model can make clear the behaviour of buried pipelines even under a high level of ground motion, which cannot be expressed by using past earthquake damage data. Diameter of pipes and joint characteristics give important effects to pipe fragility relationships. Generally speaking, DIP-A,

DIP-K and DIP-T have less seismic reliability in that order and CIP is the most vulnerable pipe material.

- The pipeline resists the ground motions by pipe displacement for tension force and by joint rigidity for compressive forces. Then these maximum axial forces are corresponding to compressive forces.
- The pipeline failure under a high level of ground motion is the discontinuous damage process of joints and the pipe fragility relationship becomes constant due to the limitation of the axial force applied to the pipeline.

REFERENCES

- Hosokawa, N., Watanabe, T., Shimizu, Y., Koganemaru, K., Ogawa, Y., Kitano, T. & Isoyama, R. 2001 Damage estimation formula for low pressure gas pipelines considering ground conditions under large scale earthquake. *Proceedings of the JSCE 26th Earthquake Engineering Symposium*, pp. 1333–1336 (in Japanese).
- Isoyama, R., Ishida, E., Yune, K. & Shirozu, T. 1998 Seismic damage estimation procedure for water pipes. *10th Japan Symposium on Earthquake Engineering*, pp. 3175–3180 (in Japanese).
- Japan Gas Association 1982 *Seismic Design Guideline for Gas Pipelines*, Japan Gas Association, Tokyo (in Japanese).
- JWWA (Japan Water Works Association) 1996 *Damage and Analysis of Water Pipelines at the 1995 Hyogo-ken Nanbu Earthquake*, JWWA, Tokyo (in Japanese).
- JWWA (Japan Water Works Association) 1997 *Seismic Design Guideline and Commentary*, JWWA, Tokyo (in Japanese).
- Takada, S., Miyajima, M., Yoda, M., Fujiwara, M., Suzuki, Y. & Toshima, T. 2001 Study on the damage prediction method of buried pipelines under near field earthquake disaster. *Jpn Water Works Assoc. J.* **798**, 21–37. (in Japanese).
- Takada, S., Ivanov, R. & Morita, N. 2003 Large deformation analysis of jointed pipelines by DEM. *Mem. Constr. Eng. Res. Inst. Found.* **45**, 111–122. (in Japanese).

First received 30 September 2009; accepted in revised form 20 January 2010